Causal pulses with rectangular spectral content: a tool for TD analysis of uwb antenna performance

Lager, IE; de Hoop, AT

Important note
To cite this publication, please use the final published version (if applicable).
Please check the document version above.

Causal Pulses With Rectangular Spectral Content: A Tool for TD Analysis of UWB Antenna Performance

Ioan E. Lager, *Member, IEEE*, and Adrianus T. de Hoop, *Member, IEEE*

Abstract—A class of causal model pulses is constructed by applying a causal modulation to a noncausal function with a rectangular spectral diagram. A particularly suitable modulation is the power exponential pulse, the resulting model pulse having a spectral behavior that is practically flat over a controllable bandwidth, with a steep falloff outside the band. Some of the devised pulses are opportune excitations in ultrawideband antenna models, thus representing effective instruments in their performance analysis, and are appropriate as inputs in electromagnetic time-domain simulation packages.

Index Terms—Performance analysis, time-domain analysis, ultrawideband antennas.

I. INTRODUCTION

ULTRAWIDEBAND (UWB) antennas are instrumental to pursuing the evolution in wireless applications [1]. Their increasingly sophisticated designs place high demands on the electromagnetic (EM) characterization tools used for their performance prediction. To this end, due to their suitability for UWB investigations, *time-domain* (TD) approaches are at the core of a steadily increasing number of such tools [2]–[5].

A prime ingredient in EM TD analyses are the model pulses exciting the configurations. They must be consistent with a fundamental property of any physical system, i.e., the *causality* of its behavior (the property that its action vanishes prior to the action of the (field) generating sources). This property is essential for ensuring the physical realizability of any pulse [6, p. 607]. Additionally, the behavior of the EM field radiated by noncausal sources in unbounded domains [7, pp. 816–817] implies that using noncausal exciting pulses is detrimental for the antenna design and analysis. Furthermore, although the frequency-domain (FD) behavior is not relevant from a TD analysis perspective, pulses with a flat spectral diagram over a certain frequency band are preferable for reasons of compatibility with measurement equipment capabilities (network analyzers have sources with a flat spectral diagram) and for establishing correspondences with traditional concepts in antenna engineering, e.g., the operational bandwidth.

Many studies employ Gaussian pulses (or their derivatives), e.g., [2] and [3], or the square root raised cosine (SRRC) pulse, e.g., [4] and [5], as model excitations. Such pulses violate the causality condition. Alternatively, [8] presented a family of model pulses whose mathematical form explicitly takes causality into account. Those pulses allow mimicking actual pulse shapes that arise from measurements carried out on integrated circuits. However, their spectral diagram does not contain any (almost) flat region.

This letter discusses a modality to construct causal model pulses that conform to the two requirements mentioned above. The most adequate results will be obtained by modulating a sinc-cosine function by means of a power exponential pulse [8]. The resulting model pulses will be shown to have a practically flat spectral diagram over a bandwidth that can be controlled via a small number of parameters, with a steep falloff outside that band. In this manner, they are requisite to developing UWB antenna models and for the performance analysis of existing ones. Furthermore, they are suitable as excitation signatures in EM TD simulation packages.

II. PREREQUISITES

The tool of investigation in this study is the one-sided time Laplace transformation $\overset{\mathbf{LT}}{\longmapsto}$ where causality is incorporated in the mathematical properties of the system's transform in the complex transform-parameter plane. Note that causal pulses are analytic in the right half of that plane and have pole singularities in that plane's left half. Given a real-valued, causal (electrical) quantity $F(t)$ (with t being the time coordinate)

$$\hat{F}(s) = \int_{t=0}^{\infty} [\exp(-st)F(t)]\,\mathrm{d}t, \qquad \text{for } s \in \mathbb{C},\ \mathrm{Re}(s) > 0. \quad (1)$$

The Fourier transformation $\overset{\mathbf{FT}}{\longmapsto}$ follows from (1) taking $s = \mathrm{j}\omega = \mathrm{j}2\pi f$, with $\omega \in \mathbb{R}$ being the angular frequency and $f \in \mathbb{R}$ the frequency. The real-valuedness of $F(t)$ implies that

$$\hat{F}(-\mathrm{j}\omega) = \hat{F}^*(\mathrm{j}\omega) \quad (2)$$

where $*$ denotes complex conjugation.

III. SIGNALS WITH RECTANGULAR SPECTRAL DIAGRAMS

The spectral behavior of causal field quantities $F(t)$ is, in accordance with Parseval's theorem, described by the *energy spectral density* $|\hat{F}(\mathrm{j}\omega)|^2$. In view of the objectives stated in the Introduction, we look for signals whose spectral behavior's shape follows closely a *rectangular spectral diagram* that, for a frequency band $[f_\mathrm{l}, f_\mathrm{h}]$, $0 < f_\mathrm{l} < f_\mathrm{h}$, with center frequency $f_\mathrm{c} = (f_\mathrm{l} + f_\mathrm{h})/2$ and bandwidth $B = f_\mathrm{h} - f_\mathrm{l}$, is

$$|\hat{F}(\mathrm{j}\omega)| = W^{\frac{1}{2}}\Pi\left(\omega - 2\pi f_\mathrm{c}, 2\pi B\right) \quad (3)$$

in which W is the energy spectral density level and

$$\Pi(x, x_\mathrm{w}) \overset{\mathrm{def}}{=} H(x + x_\mathrm{w}/2) - H(x - x_w/2)$$

$$\text{for } x, x_\mathrm{w} \in \mathbb{R},\ x_w > 0 \quad (4)$$

is the rectangle function, with $H(\cdot)$ being the Heaviside unit step function. By making use of (2), the Fourier transform of a signal whose spectral behavior is the one in (3) is

$$\hat{F}(\mathrm{j}\omega) = W^{\frac{1}{2}}[\Pi(\omega, 2\omega_\mathrm{h}) - \Pi(\omega, 2\omega_\mathrm{l})] \qquad (5)$$

with $\omega_\mathrm{l} = 2\pi f_\mathrm{l}$ and $\omega_\mathrm{h} = 2\pi f_\mathrm{h}$. Application of the inverse Fourier transform in (5) yields

$$F(t) = \frac{1}{2\pi} \int\limits_{\omega=-\infty}^{\omega=\infty} W^{\frac{1}{2}}[\Pi(\omega, 2\omega_\mathrm{h}) - \Pi(\omega, 2\omega_\mathrm{l})]\mathrm{d}\omega$$

$$= 2BW^{\frac{1}{2}}\mathrm{sinc}(Bt)\cos(2\pi f_\mathrm{c}t) \qquad (6)$$

in which $\mathrm{sinc}(x) \overset{\mathrm{def}}{=} \sin(\pi x)/(\pi x)$, for $x \in \mathbb{R}$. Based on this, a signal with a rectangular spectral diagram has the expression

$$G(t) = \mathrm{sinc}[B(t - t_0)]\cos[2\pi f_c(t - t_0)] \qquad (7)$$

in which we included a possible time shift t_0 (henceforth, we take $t_0 \geqslant 0$). Its Fourier transform is

$$\hat{G}(\mathrm{j}\omega) = \frac{\exp(-\mathrm{j}\omega t_0)}{2B} \begin{cases} 1, & \text{for } \omega_\mathrm{l} < |\omega| < \omega_\mathrm{h} \\ 0, & \text{otherwise.} \end{cases} \qquad (8)$$

Nevertheless, $G(t)$ is noncausal and, thus, is not acceptable for our purposes. For constructing a causal model pulse, this function is then modulated by a *causal pulse* $M(t)$ as

$$S(t) = M(t)G(t). \qquad (9)$$

Since the Fourier transform of $S(t)$ is obtained by applying the convolution theorem [9, p. 115], the spectral behavior of this signal will deviate from the rectangular one.

Hereafter, a number of modulation choices will be examined. The goal is to contrive causal pulses with a maximally flat behavior in the bandwidth B and a steep falloff at f_l and f_h. Furthermore, for ensuring time differentiability, no jump discontinuities will be allowed at the pulses's onset.

IV. Power Exponential Modulated-Sinc-Cosine Model Pulse

A convenient choice for the modulation in (9) is the three-parameter IEC 60050-IEV normalized *power exponential (PE) pulse* defined as [8]

$$P(t) = A(t/t_\mathrm{r})^\nu \exp[-\nu(t/t_\mathrm{r} - 1)]H(t) \qquad (10)$$

where A is the pulse amplitude, $t_\mathrm{r} > 0$ the pulse rise time, and $\nu > 0$ the pulse rising power. Its Laplace transform is

$$\hat{P}(s) = At_\mathrm{r}\frac{\Gamma(\nu+1)\exp(\nu)}{(st_\mathrm{r}+\nu)^{\nu+1}} \qquad \text{for } s \in \mathbb{C}, \ \mathrm{Re}(s) \geqslant \nu/t_\mathrm{r} \quad (11)$$

with $\Gamma(\cdot)$ denoting the Euler gamma function. The corresponding Fourier transform follows by taking $s = \mathrm{j}\omega$.

With these choices, the *power exponential modulated-sinc-cosine (PE-sinc-cosine) model pulse* is defined as

$$U(t) = A(t/t_\mathrm{r})^\nu \mathrm{sinc}[B(t - t_\mathrm{r})]\cos[2\pi f_\mathrm{c}(t - t_\mathrm{r})]$$
$$\exp[-\nu(t/t_\mathrm{r} - 1)]H(t). \qquad (12)$$

For simplicity, we confine ν to integer values. Furthermore, we interrelate B and t_r via

$$t_\mathrm{r} = K_\mathrm{sc}/B, \qquad \text{with } K_\mathrm{sc} = 1, 2, 3, \ldots. \qquad (13)$$
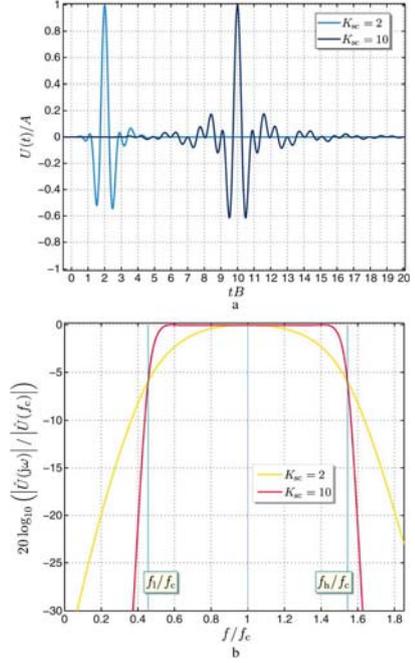
Fig. 1. Examples of PE-sinc-cosine pulses for $K_\mathrm{sc} = 2$ ($t_\mathrm{r} = 2/B$) and $K_\mathrm{sc} = 10$ ($t_\mathrm{r} = 10/B$), and $\nu = 5$. (a) Normalized time signature. (b) Normalized spectral behavior.

The Fourier transform of $U(t)$ is obtained by applying the convolution theorem,[1] yielding

$$\hat{U}(\mathrm{j}\omega) = \frac{1}{2\pi}\left[\hat{P}(\mathrm{j}\omega) \overset{(\mathrm{j}\omega)}{*} \hat{G}(\mathrm{j}\omega)\right]$$

$$= A\frac{\exp(-\mathrm{j}\omega t_\mathrm{r})}{4\pi B}$$
$$\times \left[\mathcal{I}_{\hat{U}}(\omega - \omega_\mathrm{h}, \omega - \omega_\mathrm{l}) + \mathcal{I}_{\hat{U}}(\omega + \omega_\mathrm{l}, \omega + \omega_\mathrm{h})\right] \qquad (14)$$

where $\overset{(\mathrm{j}\omega)}{*}$ denotes frequency convolution and

$$\mathcal{I}_{\hat{U}}(\omega_\mathrm{i}, \omega_\mathrm{f}) = \int\limits_{\omega_\mathrm{i}}^{\omega_\mathrm{f}} [\exp(\mathrm{j}\omega' t_\mathrm{r})\hat{P}(\mathrm{j}\omega')]\mathrm{d}\omega'$$

$$= A\left(\exp(\nu)\int\limits_{t_\mathrm{r}\omega_\mathrm{i}}^{t_\mathrm{r}\omega_\mathrm{f}}\frac{\exp(\mathrm{j}\xi)}{\mathrm{j}\xi+\nu}\mathrm{d}\xi\right.$$

$$\left.+\mathrm{j}\sum_{m=1}^{\nu}\left\{\Gamma(m)[\exp(\alpha)\alpha^{-\nu+m-1}]|_{\alpha_\mathrm{i}}^{\alpha_\mathrm{f}}\right\}\right) \qquad (15)$$

with $\{\alpha_i = \mathrm{j}t_\mathrm{r}\omega_\mathrm{i} + \nu\}$ and $\alpha_f = \mathrm{j}t_\mathrm{r}\omega_\mathrm{f} + \nu$.

Examples of PE-sinc-cosine normalized time signatures and corresponding normalized spectral diagrams are given in Fig. 1.[2] The spectral diagrams demonstrate the ability of the PE-sinc-cosine model pulse to approximate very well the targeted rectangular spectral behavior.

---

[1]While it may be possible to derive analytic expressions of the Fourier transform for specific pulse parameters, the approach adopted in this work ensures the generality of the results.

[2]The reported spectral diagrams correspond to the widest subband in the FCC mask, i.e., from 3.1 until 10.6 GHz [10, Sec. K.3.6].

Since (14) contains integrals that are evaluated numerically, a detailed numerical study was conducted for understanding the influence of the parameters on the pulse's spectral behavior. For brevity, only the conclusions of this study are discussed.

1) The spectral diagram approximates increasingly well a rectangular shape as K_{sc} increases, while the influence of ν on its shape is minimal. Note that the properties of the PE pulse imply that ν does have an impact on the spectral behavior as $f \downarrow 0$, but this low-frequency behavior is irrelevant for the practical applications envisaged for our model pulses.
2) By studying the behavior of $|\hat{U}(j2\pi f_{l,h})|^2/|\hat{U}(j\omega)|^2_{\max}$ over a wide range of $K_{sc} \geqslant 3$ and $\nu \geqslant 2$ values, it was established that $|\hat{U}(j2\pi f_{l,h})|^2/|\hat{U}(j\omega)|^2_{\max} \approx 1/4$.
3) By studying the variation of the maximum spectral magnitude over a wide range of $K_{sc} \geqslant 3$ and $\nu \geqslant 2$ values, it was concluded that this quantity is, practically, constant for K_{sc} and almost independent of ν.

Based on the above observations, we now formulate some practical rules for constructing PE-sinc-cosine model pulses.

1) The diagram's flat region, its -6-dB points, and falloff outside the band are primarily controlled by K_{sc}, providing $K_{sc} \geqslant 3$. Under this condition, the parameters B and f_c follow, essentially, from the intended band's limits.
2) The pulse power ν has a limited influence on the spectral diagram's shape. It can then be chosen more or less arbitrarily, e.g., for ensuring a certain pulse "smoothness."

V. TRUNCATED SINC-COSINE MODEL PULSE

Taking $\nu = 0$ in (12) results in

$$V(t) = A \operatorname{sinc}[B(t - t_0)] \cos[2\pi f_c(t - t_0)]H(t) \qquad (16)$$

the PE pulse reducing to the Heaviside step function. Note that the generic t_0 notation was used in (16) for the time shift in the sinc-cosine function (t_r has no significance in this case). Moreover, for preventing jump discontinuities at the pulse onset, we take $t_0 = K_{sc}/B$, $K_{sc} = 1, 2, 3, \ldots$ The resulting pulse is termed as *truncated sinc-cosine (T-sinc-cosine) model pulse*, with $H(t)$ now playing the role of the modulation in (9). This choice amounts to a straightforward truncation and is frequently used in filter theory or in digital communications for ensuring the causality of the sinc-cosine function [6, p. 607]. For determining the spectral behavior of the T-sinc-cosine pulse, we start from

$$Y(t, \omega_0, t_0) = \cos[\omega_0(t - t_0)] \xmapsto{\text{LT}} \hat{Y}(s, \omega_0, t_0)$$
$$= \frac{1}{s^2 + \omega_0^2} [s \cos(\omega_0 t_0) + \omega_0 \sin(\omega_0 t_0)]$$
$$\text{for } \operatorname{Re}(s) > 0. \quad (17)$$

The Fourier transform follows taking $s = \epsilon + j\omega$, with $\epsilon \downarrow 0$ (for convenience, we write $s = j\omega$). By now using

$$\operatorname{sinc}(Bt) \xmapsto{\text{FT}} \frac{1}{B}\Pi(\omega, 2\pi B) \qquad (18)$$

the convolution theorem yields

$$\hat{V}(j\omega) = \frac{A \exp(-j\omega t_0)}{2\pi B} \left[\Pi(j\omega, j2\pi B) \overset{(j\omega)}{*} \hat{Y}(j\omega, \omega_0, t_0) \right]$$
$$= \frac{A \exp(-j\omega t_0)}{2\pi B} \mathcal{I}_{\hat{V}}(\omega - \pi B, \omega + \pi B) \qquad (19)$$
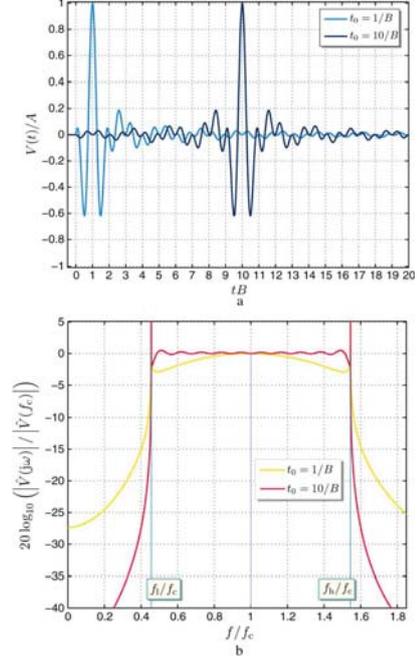

Fig. 2. Examples of T-sinc-cosine pulses for $K_{sc} = 1$ ($t_0 = 1/B$) and $K_{sc} = 10$ ($t_0 = 10/B$). (a) Normalized time signature. (b) Normalized spectral behavior.

in which

$$\mathcal{I}_{\hat{V}}(\omega_i, \omega_f) = \int_{\omega_i t_0}^{\omega_f t_0} \frac{\exp(j\xi) [j\xi \cos(\xi_0) + \xi_0 \sin(\xi_0)]}{\xi_0^2 - \xi^2} d\xi \quad (20)$$

with $\omega_{i,f} = \omega \mp \pi B$ and $\xi_0 = \omega_c t_0$. The integral in (20) must be evaluated numerically. The expression has logarithmic singularities at $f = f_l$ and $f = f_h$. The way to evaluate this integral in MATLAB is by taking $s = \epsilon' \omega_c + j\omega$, with ϵ' sufficiently small. The denominator in (20) is then adjusted by adding the term $j2\epsilon'(\omega_c t_0)\xi$. With this correction, the integral could consistently be evaluated by means of the quadl function for $\epsilon' = 10^{-10}$ (with values up to $\epsilon' = 10^{-6}$ yielding faster computations at the cost of a limited loss of accuracy).

The normalized time signature and the normalized spectral behavior of the T-sinc-cosine model pulse are exemplified in Fig. 2 for $t_0 = 1/B$ and $t_0 = 10/B$. The spectral diagrams show logarithmic singularities at f_l and f_h. Apart from these singularities, the spectral behaviors approximate increasingly well a rectangular one. Nevertheless, the singular spectral behavior drastically restricts the utility of this model pulse.

VI. TIME-WINDOWED SINC-COSINE MODEL PULSE

A third modality to ensure the causality is by taking the modulation in (9) as a time-windowed pulse

$$T_w(t, t_w) = A\Pi(t - t_w/2, t_w) \qquad \text{with } t_w > 0. \qquad (21)$$

Its Lapace transform is

$$\hat{T}_w(s, t_w) = A\frac{1 - \exp(-s, t_w)}{s}, \qquad \text{for } \operatorname{Re}(s) > 0 \qquad (22)$$

that becomes for $s = j\omega$

$$\hat{Y}_w(j\omega, t_w) = A\, t_w, \exp(-j\omega t_w/2)\operatorname{sinc}\left[\frac{\omega, t_w}{(2\pi)}\right]. \qquad (23)$$
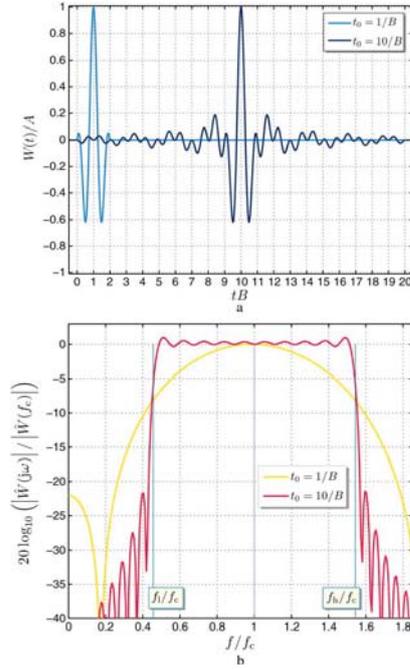
Fig. 3. Examples of TW-sinc-cosine pulses for $K_{sc} = 1$ ($t_0 = 1/B$) and $K_{sc} = 10$ ($t_0 = 10/B$). (a) Normalized time signature. (b) Normalized spectral behavior.

A convenient choice for the t_w parameter is $t_w = 2t_0$, with t_0 the time shift in (7). By substituting (21) in (9), we obtain the *time-windowed sinc-cosine (TW-sinc-cosine) model pulse*

$$W(t) = \text{sinc}[B(t - t_0)] \cos[2\pi f_c(t - t_0)] T_w(t, 2t_0). \quad (24)$$

For preventing jump discontinuities at the pulse onset, we take $t_0 = K_{sc}/B$, $K_{sc} = 1, 2, 3, \ldots$. With these choices, using the convolution theorem, it is found that

$$
\begin{aligned}
W(t) &\overset{\textbf{FT}}{\longmapsto} \hat{W}(j\omega) \\
&= \frac{1}{2\pi} \left[\hat{G}(j\omega) \overset{(j\omega)}{*} \hat{Y}_w(j\omega, 2t_0) \right] \\
&= \frac{\exp(-j\omega t_0)}{2\pi B} \left[\mathcal{I}_{\hat{W}}(\omega - \omega_h, \omega - \omega_l) + \mathcal{I}_{\hat{W}}(\omega + \omega_l, \omega + \omega_h) \right]
\end{aligned}
\quad (25)
$$

in which

$$\mathcal{I}_{\hat{W}}(\omega_i, \omega_f) = \int_{\omega_i t_0}^{\omega_f t_0} \text{sinc}\left(\frac{\xi}{\pi}\right) d\xi. \quad (26)$$

This integral can be directly evaluated numerically, the integrand being bounded for any ξ.

The normalized time signature and the normalized spectral behavior of the TW-sinc-cosine model pulse are illustrated in Fig. 3 for $t_0 = 1/B$ and $t_0 = 10/B$. The relevant spectral diagrams approximate increasingly well a rectangular one as K_{sc} increases. However, the TW-sinc-cosine model pulse can only be differentiated once, the first derivative already showing jump discontinuities at the time-window's ends, and, hence, is inadequate for pulsed-field models requiring differentiations of

orders one, two and three of the exciting pulse [7, Sections 26.9 and 26.10], [11].

It is now concluded that the PE-sinc-cosine model pulse is our best candidate for a causal pulse with an approximately rectangular spectral diagram. Depending on the situation at hand, the TW-sinc-cosine model pulse may also be a convenient solution. Due to its singular spectral contents, the T-sinc-cosine model pulse is deemed inadequate.

VII. CONCLUSION

A manner for constructing *causal* model pulses with a rectangular spectral content was examined. By starting from a noncausal sinc-cosine function with a rectangular spectral diagram, three kinds of modulations for ensuring the model pulse's causality were experimented with. The most effective modulation was that by means of a power exponential pulse, the resulting *power exponential modulated-sinc-cosine model pulse* having a spectral behavior that is practically flat over a controllable bandwidth, with a steep falloff outside the band. Alternatively, the *time-windowed, sinc-cosine model pulse* also has an adequate spectral diagram, but is less widely applicable since it can be time-differentiated only once. A third modality, by truncating the sinc-cosine function, yielded a model pulse with a singular spectral behavior, this drastically limiting its utility.

The PE-sinc-cosine and (in some cases) TW-sinc-cosine model pulses are opportune as excitations for the design and performance analysis of UWB antennas. They can also be easily incorporated as inputs in EM simulation packages.

REFERENCES

[1] G. Adamiuk, T. Zwick, and W. Wiesbeck, "UWB antennas for communication systems," *Proc. IEEE*, vol. 100, no. 7, pp. 2308–2321, Jul. 2012.

[2] A. Shlivinski, E. Heyman, and R. Kastner, "Antenna characterization in the time domain," *IEEE Trans. Antennas Propag.*, vol. 45, no. 7, pp. 1140–1149, Jul. 1997.

[3] M. Ciattaglia and G. Marrocco, "Investigation on antenna coupling in pulsed arrays," *IEEE Trans. Antennas Propag.*, vol. 54, no. 3, pp. 835–843, Mar. 2006.

[4] A. Dumoulin and M. J. Ammann, "Differentially-fed UWB slot antenna for direct board integration," in *Proc. 6th EuCAP*, Prague, Czech Republic, Apr. 2012, pp. 765–768.

[5] A. Dumoulin, M. John, M. J. Ammann, and P. McEvoy, "Optimized monopole and dipole antennas for UWB asset tag location systems," *IEEE Trans. Antennas Propag*, vol. 60, no. 6, pp. 2896–2904, Jun. 2012.

[6] J. K. Proakis and M. Salehi, *Digital Communications*, 5th ed. New York, NY, USA: McGraw-Hill, 2008.

[7] A. T. de Hoop, *Handbook of Radiation and Scattering of Waves*. London, U.K.: Academic, 1995.

[8] I. E. Lager, A. T. de Hoop, and T. Kikkawa, "Model pulses for performance prediction of digital microlectronic systems," *IEEE Trans. Compon., Packag., Manuf. Technol.*, vol. 2, no. 11, pp. 1859–1870, Nov. 2012.

[9] R. N. Bracewell, *The Fourier Transform and Its Applications*. New York, NY, USA: McGraw-Hill, 2000.

[10] *"Manual of Regulations and Procedures for Federal Radio Frequency Management"* 2013 ed. National Telecommunications and Information Administration, May 2011 [Online]. Available: http://www.ntia.doc.gov/files/ntia/publications/redbook/2013/May_2013_Edition_of_the_NTIA_Manual.pdf

[11] I. E. Lager and A. T. de Hoop, "Loop-to-loop pulsed electromagnetic field wireless signal transfer," in *Proc. 6th EuCAP*, Prague, Czech Republic, Apr. 2012, pp. 786–790.